International Journal of ISSI, Vol. 14 (2017), No. 1, pp. 23- 29

Effects of Martensite Reversion Parameters on the Formation of Nano/ Ultrafine Grain Structure in AISI 304L Stainless Steel

H. Esfandiary [1] , S. R. Hosseini [2], F. Ashrafizadeh [3], A. Kermanpur [4]

[1, 3, 4] *Department of Materials Engineering, Isfahan University of Technology, Isfahan 84156- 83111, Iran*
[2] *Department of Materials Engineering, Maleke-ashtar University of Technology, Isfahan 83145-115, Iran*

Abstract

Formation of nano/ultrafine grain structure in AISI 304L austenitic stainless steel through the martensite reversion treatment was studied. The solution annealed specimens were cold rolled up to 95 % thickness reduction at -15 °C. The cold-rolled specimens were subjected to reversion annealing treatment at the temperature range of 700-1000 °C for 10–150 min. Microstructural evolutions were analyzed using ferritscopy, X-ray diffraction, and field emission scanning electron microscopy techniques, whereas mechanical properties were determined by the hardness test. The saturation strain during cold rolling was about 56 % reduction. The mean austenite grain size of 135 nm was obtained by 95 % cold reduction and annealing at 700 °C for 10 min. It was found that increasing cold reduction resulted in grain refinement at the same condition of reversion annealing and higher hardness.

Keywords: Nano/ultrafine; Stainless steel; Cold work; Reversion annealing.

1. Introduction

The metastable austenitic stainless steels are widely used in many industrial components. These materials exhibit superior corrosion resistance, good high- and low-temperature strength and high ductility. However, their yield strength is relatively low in the annealed condition [1)]. Grain refinement, solid solution strengthening, and work hardening are mechanisms that increase strength of stainless steels and keep the mentioned features simultaneously. Among these methods, grain refinement is able to improve both strength and toughness [2- 4)]. Nanostructured and ultrafine grained polycrystalline materials fabricated by thermo-mechanical processing have shown an increase in strength 5 to 10 times higher than their the coarse grained counter parts [5)]. The martensite reversion thermo-mechanical process involves heavily cold rolling and subsequent annealing to convert the strain-induced martensite to the ultrafine grained austenite. Alloy composition, thickness reduction, temperature and time for complete reversion transformation are the main factors for fabrication of the nanostructured and ultrafine grained metastable austenitic stainless steels [5)]. These materials have low stacking fault energy [6)], and thus bundles of faults readily form during cold deformation. The strain induced nucleation of α′-martensite primarily occurs at slip bands and is associated with a high density of dislocation pile-ups [5)]. In order to form α′-martensite, cold work must be applied above the martensite start temperature (M_s) and below M_d [7)]. It should be noted that the martensite fragmentation during deformation produces a large number of crystal defects in the structure and provides nucleation sites for austenite during reverse transformation, leading to noticeable grain refinement [8)].

Up to now, many studies have been conducted on the influence of cold reduction and reversion annealing parameters on the grain refinement in many groups of austenitic stainless steels [9- 13)].

In this work, the effects of temperature and various percent of cold deformation and reversion parameters on the formation of grain structure in the AISI 304

** Corresponding author*
Tel: +98 31 33915738, Fax: +98 31 33912752
Email: h.esfandiary@ma.iut.ac.ir
Address: Department of Materials Engineering, Isfahan University of Technology, Isfahan 84156- 83111, Iran
1. M.Sc.
2. Assistant Professor
3. Professor
4. Professor

stainless steel are investigated. In the previous works the effect of limited range of thickness reductions (90 %) at room temperature on the austenite to strain-induced martensite transformation have been investigated [14,15]. However, in the present work, the effect of a wide range of thickness reductions (10–95 %) at -15 °C on the austenite to strain-induced martensite transformation were investigated, and the microstructure and mechanical properties of the reversion annealed specimens were characterized.

2. Materials and Methods

Commercial grade sheet form of AISI 304L austenitic stainless steel was used as a primary material for experimental tests. Table 1 lists the chemical composition of the as-received material. Specimens with the size of 100 mm × 30 mm × 10 mm were cut and solution annealed for 2 h at 1000 °C, then quenched immediately in water. The optical micrograph of the solution annealed is illustrated in Fig. 1. As can be seen, the microstructure is consisted of γ-austenite, and a very low amount of the retained δ-ferrite which is formed along the grain boundaries.

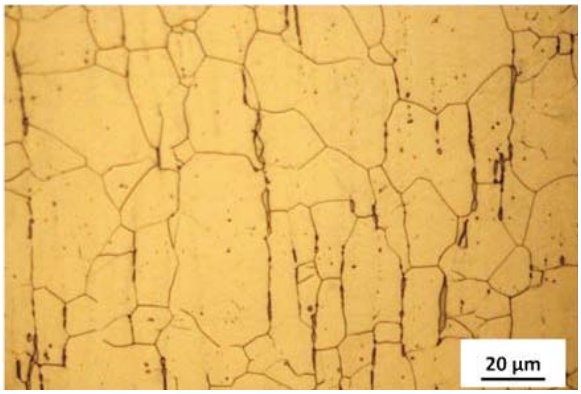

Fig. 1. The optical micrograph of the solution annealed specimen, 2 h/1000 °C.

Stability of austenite under plastic deformation depends on the M_S (the temperature below which austenite transforms spontaneously to martensite), $M_{d\,30/\,50}$ (the temperature at which 50 % of the strain induced martensite is produced after 30 % true deformation under tensile condition) and stacking fault energy (SFE). Therefore, M_S and $M_{d\,30/50}$ were calculated using the equations proposed by "Eichelmann and Hull" and "Angeline and Nohara", respectively [11]. The SFE is determined by the composition of the austenitic stainless steels at the cold deformation temperature according to "Schramm and Reed" equation [12]. Calculated M_S , $M_{d\,30/\,50}$, SFE as well as average grain size and hardness of annealed specimens before cold work, were shown in Table 2.

$$M_S(°C) = 1305 - \left[1667 \times (\%C + \%N) + 28 \times (\%Si) + 33 \times (\%Mn) + 42 \times (\%Cr) + 61 \times (\%Ni)\right] \quad \text{Eq. (1)}$$

$$M_{d30}(°C) = 413 - \left[462 \times (\%C + \%N) + 9.2 \times (\%Si) + 8.2 \times (\%Mn) + 13.7 \times (\%Cr) + 9.5 \times (\%Ni) + 18.5 \times (\%Mo)\right] \quad \text{Eq. (2)}$$

$$M_{d30}(°C) = 551 - 13.7(\%Cr) - 29(\%[Ni + Cu]) - 8.1(\%Mn) - 18.5(\%Mo) - 9.2(\%Si) - 68(\%Nb) - 462(\%[C + N]) - 1.42(GS - 8) \quad \text{Eq. (3)}$$

$$SFE(mj/m^2) = -53 + 0.7(\%Cr) + 6.2(\%Ni) + 3.2(\%Mn) + 9.3(\%Mo) \quad \text{Eq. (4)}$$

Table 1. Chemical composition of used AISI304L austenitic stainless steel.

Element	C	Cr	Ni	Mo	Mn	Si	P	S	Cu	Fe
(wt. %)	0.026	18.30	8.00	0.15	1.24	0.32	0.024	0.005	0.13	Base

Table 2. Calculated martensite transformation temperatures, stacking fault energy for used AISI 304L.

M_S (°C)	$M_{d\,30/50}$ (°C)		SFE (mj/m^2)	ASTM grain size
Eichelman and Hull (1953)	Angel (1954)	Nohara et al.(1977)	Schramm and Reed (1975)	
-45	58	36	15	8

The multi-pass unidirectional cold rolling was carried out by a two-high rolling mill under oil lubrication. Different thickness reductions from 10 to 95 % with 0.5 %, were applied on the specimens in each pass with inter-pass cooling at -15 ± 3 °C using ice, methanol and water. A schematic representation of the process is shown in Fig. 2. The reversion of martensite to austenite in the 80 and 95 % cold rolled specimens were carried out by an isothermal annealing in the temperature range of 700–1000 °C for different times. The Amounts of cold work, annealing durations and temperatures are presented in Table 3.

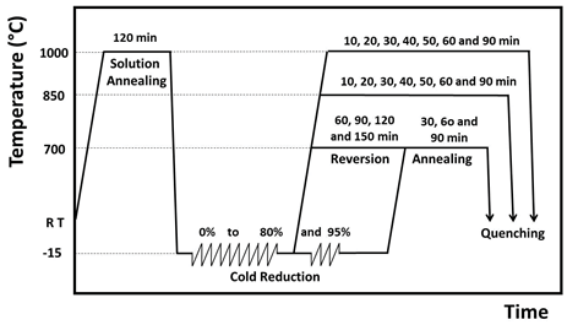

Fig. 2. Schematic diagram of thermo-mechanical process to evaluate final austenite average grain size.

Table 3. Parameters of reversion annealing at different cold reduction.

Cold reduction (%)	Annealing Temperature (°C)	Annealing Time (min)
95	700	10
95	700	30
95	700	60
95	700	90
80	700	60
80	700	90
80	700	120
80	700	150
80	850 and 1000	10
80	850 and 1000	20
80	850 and 1000	30
80	850 and 1000	40
80	850 and 1000	50
80	850 and 1000	60
80	850 and 1000	90

To reveal the microstructure, specimens were mounted in resin and ground with SiC emery papers from 80 grit down to 2400 grit. Then all specimens were electro etched with 63.5 % nitric acid. The etching was carried out at 0.9V for about 610-second for specimens with 95 % and about 60600-second for specimens with 80 % cold reduction. The microstructures were revealed by optical, scanning electron microscope (SEM Philips XL230, with Magn 15.00 Kx) and field emission scanning electron microscope (FESEM MIRA 3XM TESCAN, with Magn 30.00 Kx). For the grain size measurements the linear intercept method was used which is described in detail in section 13 of ASTM standard E 11296-. Phase identification was performed using X-ray diffraction technique (Philips X' Pert, Cu Kα anode, $\lambda = 0.154184$ nm, $2\theta = 20 – 100$ degree and exposure time 10 min). In some specimens, to remove the surface martensite that induced by mechanical polishing was used from electropolish at 30 V for 30 s by using electrolyte 200 ml perchloric acid and 800 ml ethanol. Magnetic technique using Feritscope (Helmut Fischer GmbH, model MP3E-S), was used for the determination of α´-martensite phase after cold rolling and reversion annealing. The device was calibrated with δ-ferrite standard samples. The results were adapted to the α´-martensite contents with the correlation factor of 1.7 [13]. The hardness was determined using Vickers hardness tester (Wilson Wolpert tester 930250/ universal hardness machine) with the indenting load of 98 N load.

3. Results and Discussion

3. 1. Formation of α´-martensite

Fig 3. shows the volume fraction of the strain induced martensite versus the total cold reduction. The resulting transformation curve has a sigmoidal shape. The volume fraction of strain induced martensite enhanced by the increase of cold work percentage. These results agree with the other studies of the influence of varying degrees of cold deformation [4, 14, 15]. It can be seen during 40 % thickness reduction, more than 90 vol.% of austenite transformed to α´-martensite, while it was almost completely transformed by applying 50% cold work at 0 °C [14]. Decreasing super saturation of α´-martensite with decreasing rolling temperature is attributed to the decrease in the stacking fault energy (SFE) and consequently increasing the available chemical driving force for the transformation. The SFE plays an important role in the austenite stability, since it controls the formation of the shear bands, and thus the formation of nucleation sites for the ά-martensite [16]. When transformation completes, further cold work results in the increase of density of crystal defects such as dislocation tangles, stacking faults, shear bands and mechanical twins in the structure [17].

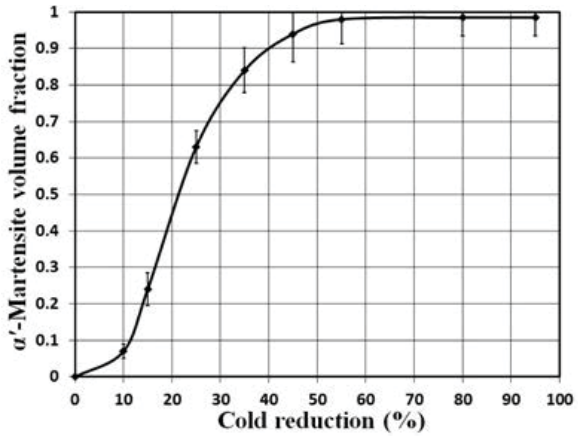

Fig. 3. The effect of thickness reduction on the volume fraction of α′-martensite

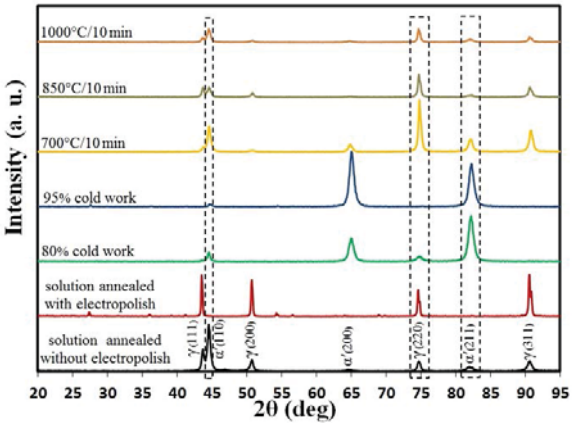

Fig. 4. Comparative X-ray diffraction patterns for different processes

3. 2. X-ray diffraction results

The X-ray patterns of the solution annealed, 80 and 95 % cold rolled and reversion annealed specimens are depicted in Fig. 4. As it is observed, the solution annealed specimen exhibits primarily austenite peaks along with the (1 1 0), (2 0 0) and (2 1 1) martensite peaks. Since austenite is metastable, therefore, induced martensite was created at the surface by thermal shock in quenching and mechanical stress when specimen prepared to analysis. X-ray diffraction pattern of solution annealed and electropolished, revealed that martensite peaks were disappeared in Fig 4. With performing cold reduction, the austenite gradually was decreased and finally the microstructure was changed to fully α′-martensite. When the cold working were done with 80 and 95 % reduction, the microstructures change to fully α′-martensite.

Upon the reversion annealing in the range of 700–1000 °C, the α′-martensite reverts to γ-austenite. The intensity of the γ-austenite peaks are increased with increasing the temperature. This means an increase in the volume fraction of γ-austenite. According to Fig. 4, by annealing at 700 °C for 10 min the microstructure mostly consisted of γ-austenite along with a small amount of retained α′-martensite. Increasing the temperature up to 1000 °C, would result in reversion of almost all the martensite to the austenite. In addition, an increase in the annealing temperature resulted in different types of texture in structure. It is however to be pointed out that upon annealing at 700 °C the γ reversed austenite is shifted towards the (2 0 0) planes. This shifting becomes less at temperatures above 700 °C. On the other hand, the γ-austenite phase maintains the γ (220) plains the preferred orientation when reversion temperature decreases from 1000 to 700 °C.

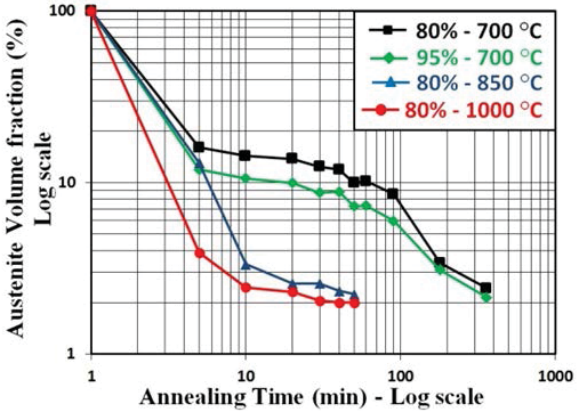

Fig. 5. α′-martensite volume fraction as a function of annealing time and temperature

3. 3. Reversion of induced α′-martensite

Reversion of austenite from α′-martensite that was analyzed by Feritscope is presented as a function of annealing time in Fig 5. As expected, the kinetics of the martensite reversion (negative slope of graph) increased with increasing the annealing temperature and cold reduction. The Complete reversion was occurred at 700, 850, and 1000 °C after 90, 5, and 2 min for specimens with 80 % cold reduction, respectively. At the temperatures above 850 °C most of the induced martensite was reverted at the beginning of the annealing process. While at the lower temperatures, martensite transformation occurred with more delay. As well as the result implies, complete reversion at low temperatures occurs in the specimens with more cold reduction. For example, in the specimens with 80 and 95 % cold reduction, the complete reversion annealing time reduced from 90 to 30 min.

This is due to formation of high density of dislocation pile-ups which increase the nucleation frequency of reversed austenite, and facilitates the formation of fine austenite grains.

Fig. 6 shows the FESEM microstructures of 95 % cold-rolled and isothermally annealed specimens with different holding times at 700 °C. The annealed specimen exhibits typical equiaxed austenite grains whose average grain size are about (135 ± 40 nm), (280 ± 45 nm), (430 ± 55 nm), and (510 ± 45 nm) revealed in Fig. 6 (a, b, c and d), respectively. The FESEM microstructure of specimens were 80 % cold worked and annealed at 700 °C for 60 min, 90 min, 120 min, and 150 min was showed in Fig. 7. The average grain size of these specimens is (775 ± 60 nm), (1160 ± 90 nm), (1300 ± 60 nm – 3200 ± 250 nm), and (3200 ± 300 nm), respectively. Furthermore, a few optical microscopy photos of 80 % cold worked and reversion annealed in different times and temperatures are compared with each other in Fig. 8

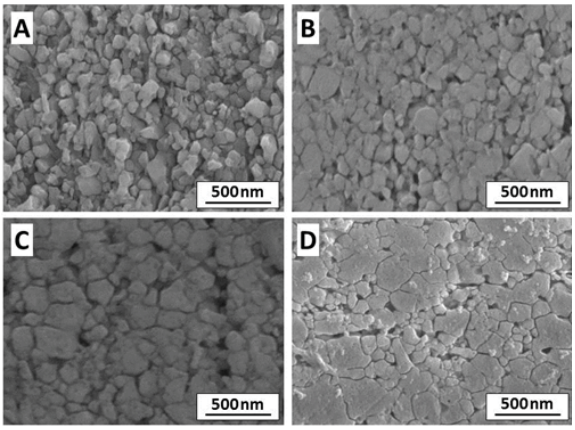

Fig. 6. FESEM of specimens annealed at (A) 700 °C/10 min, (B) 700 °C/30 min, (C) 700 °C/60 min, and (D) 700 °C/90 min with 95 % cold reduction.

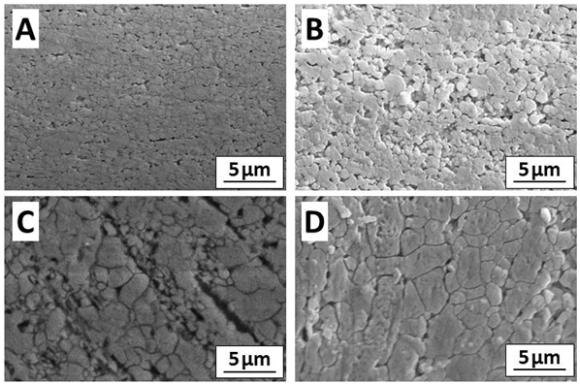

Fig. 7. FESEM of specimens annealed at (A) 700 °C/60 min, (B) 700 °C/90 min, (C) 700 °C/120 min, and (D) 700 °C/150 min with 80 % cold reduction.

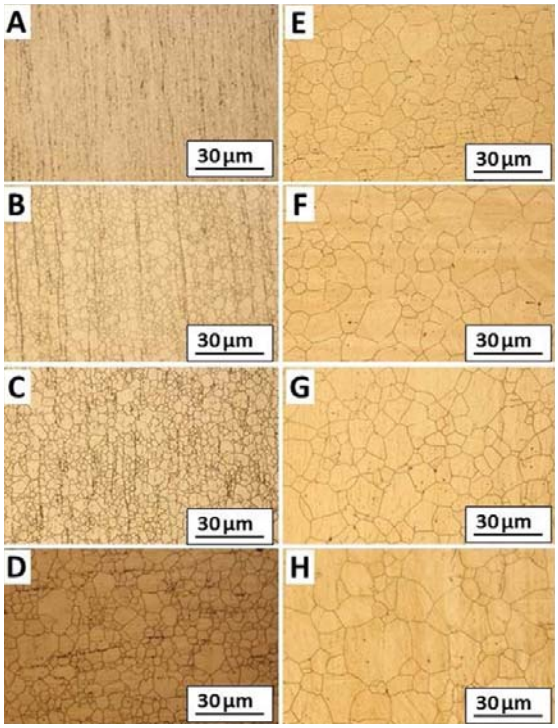

Fig. 8. Optical micrograph of specimens annealed at (A) 850 °C/10 min, (B) 850 °C/30 min, (C) 850 °C/60 min, (D) 850 °C/90 min, (E) 1000 °C/10 min, (F) 1000 °C/30 min, (G) 1000 °C/60 min, and (H) 1000 °C/90 min with 80 % cold reduction.

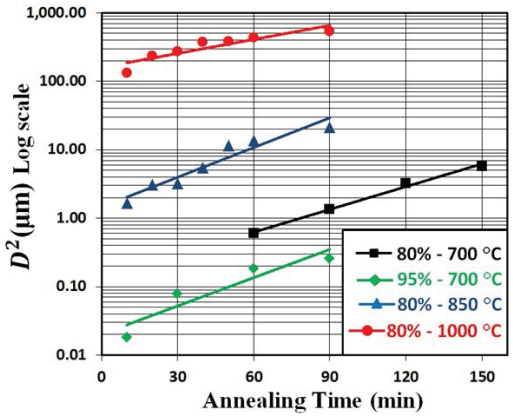

Fig. 9. Effect of annealing temperature and time on the grain size of reversed austenite.

According to these results, the diagram of grain size versus annealing time was driven in Fig. 9. As expected, the grain size of the reversed austenite increased with increasing the annealing time. This figure clearly shows that the grain growth was taken place very fast at 850 and 1000 °C. For instance, specimens that annealed at 850 °C showed a rapid grain growth from 1.3 to 4.6 µm when the annealing time was increased from 10 to 90 min; while the

samples annealed at 1000 °C, exhibited grain growth from 11.5 μm to 23 μm at the same annealing time.

In austenitic stainless steels, reversion transformation characteristics are varying from one to another. It depends on chemical compositions, cold reduction, reversion annealing parameters (temperature and time) and type of reversion (diffusional or martensitic shear type) [18]. At first, the mechanism of reversion transformation during continuous heating, is diffusionlessly and then proceeds by diffusive nucleation and growth manner during isothermal holding [8]. In general, specimens that annealed at the 700 °C with 80 and 95 % cold reduction gave a mixed microstructure of very fine reverted grains and retained martensite. 95 % cold reduction led to the formation of a larger number of reverted γ nuclei and create significantly finer nanometer to sub micrometer sized austenite grains (135, 280, 430 and 510 nm) in comparison to the 80 % cold reduction specimens. Two austenite morphologies have been reported by Misra et al [18], increasing cold reduction caused the destruction of lath martensitic structure, resulting in the formation of dislocation-cell structure and ultimately leading to finer equiaxed γ grains on reversion. The reversion kinetics were found strongly dependent on the prior cold rolling reduction and annealing conditions, and were extremely fast above 850 °C. These γ grains gradually grow with increasing the annealing time and this leads to the increase in the γ volume fraction. A small amount of tempered α′ (α'_T) which remained in the structure at 700 °C can be found within γ grains even after 150 min annealing. Most α'_T particles are located in the corner of three- and four-grain junctions of reversed γ and these might act as the obstacles against the grain growth of reversed austenite [19]. However, increasing the temperature to 850 and 1000 °C resulted in a mixture of mostly reverted austenite grains and less amount of α'_T that makes the growth of grains.

3. 4. Mechanical properties

The hardness value of the solution annealed specimen was about 190 HV_{10}, while after 80 and 95 % thickness reduction it reached to about 460 and 495 HV_{10}, respectively. The high hardness value was related to the transformation of austenite to α′-martensite and increasing the concentration of lattice defects inside the strain induced martensite. The effect of reversion annealing the temperatures and times on the hardness of annealed specimens is shown in Fig. 10. The cause of change in the hardness value with increasing the temperature and time attributed to the effect of the reversed austenite, recovery, recrystallization of hardened austenite, lower density of dislocations, lower volume fraction of martensite and grain growth of reversed austenite in the structure.

As anticipated, the rate of hardness loss in reversion annealed specimens increased with increasing the annealing temperature and time. In addition, in specimens which were cold worked to 95 %, the hardness loss in reversion annealing was less than specimens were cold worked to 80 %. The maximum rate of hardness loss in specimens corresponded to the annealing temperature of 1000 °C and after 90 min with 80 % cold work. The hardness value of 150 HV_{10} was obtained for this specimen which was less than the hardness value of the solution annealed specimen (190 HV_{10}). It is related to the difference of grain size between these two specimens (31 μm and 23 μm). The minimum rate of hardness loss was related to 700 °C and for 10 min after 95 % cold work. The hardness value of 445 HV_{10} was obtained for this specimen which was about two times higher than that of the unprocessed specimen. It is necessary to mention the Hall–Petch relationship when mechanical properties and grain size are considered. In terms of hardness, the Hall–Petch relationship is explained by Eq. (5):

$$HV = HV_0 + kD^{-0.5} \qquad \text{Eq. (5)}$$

, where HV_0 is a constant which depends on the hardness of a single crystal, D is the average austenite grain size, and k is a constant for a material with a single phase. Hall–Petch relationship between austenite grain size and hardness is shown in Fig. 11. This figure clearly shows the hardness linearly increases with increasing in $D^{-0.5}$. It can be seen that the Hall–Petch behavior holds down to at least 135 nm of grain size. These results are in agreement with the measurements on AISI 304L austenitic stainless steel that has been carried out by Forouzan et al. [14] and Huang et al. [20].

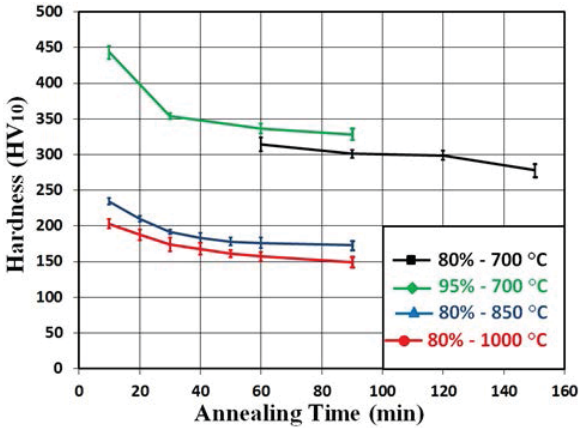

Fig. 10. Dependence of hardness versus annealing conditions.

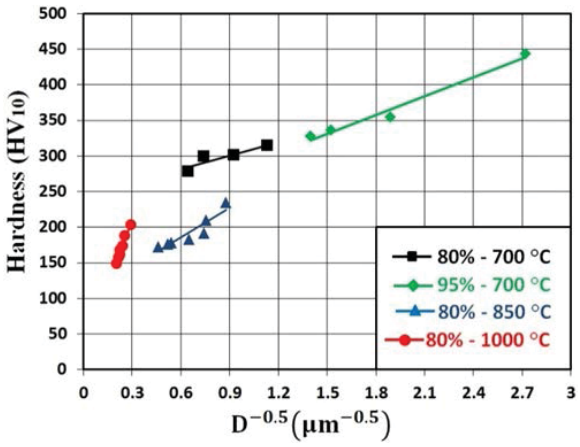

Fig. 11. Dependence of austenite grain size and hardness.

4. Conclusions

Different cold reductions were carried out on AISI304L austenitic stainless steel and the effect of the annealing temperature and time was evaluated on microstructural features and hardness. According to the findings of the present research, the following conclusions were drawn:

• The metastable austenite was almost completely transformed to α′-martensite by 40 % cold reduction at -15 ± 2 °C by strain rate of 0.5 s^{-1} and reduction in thickness of 0.1 mm per each pass.

• By increasing cold reduction from 80 to 95 %, reversion annealing happened in the lower temperatures.

• There was a good correlation between increasing cold reduction and grain size refining. The smallest austenite grain size (135 ± 40 nm) was created by 95 % cold reduction and reversion annealing at 700 °C for 10 min.

• The effect of grain size on hardness conforms to a Hall–Petch dependency in the entire range of the analysis.

• Decreasing the cold reduction and the annealing temperature and time led to a decrease in the hardness. The maximum hardness of 495 HV10 corresponded to the minimum grain size (135 ± 40 nm).

References

[[1] R. Song, D. Ponge, D. Raabe, J. Speer, D. Matlock: Mater. Sci. Eng. A., 441(2006), 1.
[2] M. Somani, P. Juntunen, L. Karjalainen, R. Misra, A. Kyröläinen, Metall. Mater. Tran. A., 40(2009), 744.
[3] M. A. Meyers, A. Mishra, D. J. Benson: Prog. Mater. Sci., 51(2006), 427.
[4] A. Rezaee, A. Najafizadeh, A. Kermanpur, M. Moallemi, Mater. Design., 32(2011), 4437.
[5] M. Eskandari, A. Kermanpur, A. Najafizadeh: Mater. Lett., 63(2009), 1442.
[6] Y. Shen, X. Li, X. Sun, Y. Wang, L. Zuo: Mater. Sci. Eng. A., 552(2012), 514.
[7] B. R. Kumar, B. Mahato, S. Sharma, J. Sahu, Metall. Mater. Tran. A., 40(2009), 3226.
[8] S. J. Lee, Y. M. Park, Y. K. Lee: Mater. Sci. Eng. A., 515(2009), 32.
[9] S. Tavares, D. Gunderov, V. Stolyarov, J. Neto: Mater. Sci. Eng. A., 358(2003), 32.
[10] K. Tomimura, S. Takaki, Y. Tokunaga: ISIJ. Int., 31(1991), 1431.
[11] A. Poulon, S. Brochet, J. B. Vogt, J. C. Glez, J. D. Mithieux: ISIJ. Int., 49(2009), 293.
[12] R. Schramm, R. Reed: Metall. Tran. A., 6(1975), 1345.
[13] J. Talonen, P. Aspegren, H. Hänninen: Mater. Sci. Tec., 20(2004), 1506.
[14] F. Forouzan, A. Najafizadeh, A. Kermanpur, A. Hedayati, R. Surkialiabad: Mater. Sci. Eng. A., 527(2010), 7334.
[15] A. Hedayati, A. Najafizadeh, A. Kermanpur, F. Forouzan: J. Mater. Process. Tec., 210(2010), 1017.
[16] J. Talonen, H. Hänninen: Acta. Mater., 55(2007), 6108.
[17] R. Misra, B. R. Kumar, M. Somani, P. Karjalainen: Scr. Mater., 59(2008), 79.
[18] R. Misra, S. Nayak, S. Mali, J. Shah, M. Somani, L. Karjalainen: Metall. Mater. Tran. A., 40(2009), 2498.
[19] Y. Yagodzinskyy, J. Pimenoff, O. Tarasenko, J. Romu, P. Nenonen, H. Hänninen: Mater. Sci. Technol., 20(2004), 925.
[20] J. Huang, X. Ye, J. Gu, X. Chen, Z. Xu, Mater. Sci. Eng. A., 532(2012), 190.